Design Considerations For Remote High-Speed Pressure Measurements Of Dynamic Combustion Phenomena

Douglas L. Straub, Donald H. Ferguson
U.S. Department of Energy – National Energy Technology Laboratory, Morgantown, WV, 26505, USA

Robert Rohrssen and Eduardo Perez
West Virginia University, Morgantown, WV 26505, USA

As gas turbine combustion systems evolve to achieve ultra-low emission targets, monitoring and controlling dynamic combustion processes becomes increasingly important. These dynamic processes may include flame extinction, combustion-driven instabilities, or other dynamic combustion phenomena. Pressure sensors can be incorporated into the combustor liner design, but this approach is complicated by the harsh operating environment. One practical solution involves locating the sensor in a more remote location, such as outside the pressure casing. The sensor can be connected to the measurement point by small diameter tubing. Although this is a practical approach, the dynamics of the tubing can introduce significant errors into the pressure measurement. This paper addresses measurement errors associated with semi-infinite coil remote sensing setups and proposes an approach to improve the accuracy of these types of measurements.

Nomenclature

A	=	Cross-sectional area
c	=	Speed of sound
d	=	Diameter
J_0, J_1	=	Bessel Functions
L	=	Length
p	=	Acoustic pressure
Q	=	Reflection coefficient for a volume terminated line
R	=	Radius
V	=	Volume of pressure transducer cavity
W	=	Wave Shear Number
y	=	Propagation constant
Fr	=	Froude Friction Factor
Pr	=	Prandtl Number
α	=	Attenuation coefficient
γ	=	Ratio of specific heats
ρ	=	Density
ζ	=	Specific acoustic impedance
υ	=	Kinematic viscosity
ω	=	Angular frequency (rad/s)
Subscripts		
0, 1, 2	=	Reference stations for P_0, P_1, and P_2 (see Fig. 1 and Fig. 6)
e	=	Reference to the closed end of semi-infinite coil

I. Introduction

As gas turbine combustion systems evolve to lower pollutant emission targets, accurate measurements of dynamic combustion processes becomes increasingly important. The current goals of the U.S. Department of Energy's Turbine Program include NOx emissions of 2 parts-per-million and fuel-flexible requirements that may include hydrogen fuels produced from coal. Combustion dynamics, lean flame extinction, and flashback are some examples of combustion challenges that require high bandwidth sensors.

Typically, high-speed pressure transducers are the instrument of choice for monitoring dynamic combustion phenomena. High-speed pressure transducers have been used to monitor combustion-driven instabilities[1,2,3]; to predict the onset of combustion instabilities[4]; and to provide feedback for active control of combustion instabilities[5]. Pressure sensors have also been used to predict the onset of lean flame extinction[6] and even changes in flame anchoring.[7] In most gas turbine applications, these high speed pressure transducers are located a significant distance from the combustion chamber[1,8]. These remote sensing systems are typically used to avoid placing the sensor in the high temperature and high pressure environment near the combustion liner. In most cases, the pressure sensing system includes a mechanism (i.e., a waveguide or semi-infinite coil) to dampen acoustic reflections over the frequency range of interest. Generally speaking, the media in these waveguides are stationary (i.e., no mean flow) and the tubing diameters are small. As a result, the most important mechanisms for sound attenuation are due to the effects of viscosity and heat loss, otherwise known as visco-thermal effects.

The transfer function between the measured pressure and the actual combustor pressure can be predicted using theoretical expressions that are based on unsteady one-dimensional relations. These models can account for the geometry of the interconnecting hardware, the temperature gradients along the hardware[9] and visco-thermal losses[8]. However, Munjal[10] has shown that experimental measurements by several investigators can disagree with theoretical values by 15 to 50 percent. Additional measurements of attenuation performed by Ferrara et. al[11] for remote pressure sensing systems similar to those used in gas turbine applications indicate that in addition to the large uncertainty, the attenuation does not vary monotonically with frequency as theory suggests. It is interesting to note that the disagreement observed by Ferrara et. al[11] is of the same order as described by Munjal[10].

A. Background

Although the results of Ferrara et. al[11] were very applicable to the pressure sensing systems used in gas turbine applications, the errors associated with remote pressure measurements were not addressed. Furthermore, experimental evidence relative to these remote pressure sensing systems is difficult to find in the open literature.

Van Ommen et. al[12] describe theoretical and experimental results from a pressure sensing system for gas-solid fluidized bed applications in which the frequencies of interest are less than 200 Hertz. Although the pressure sensing system used in this work is not identical to the systems employed in gas turbine applications, Van Ommen et. al[12] show that even the best model (i.e., Bergh and Tijdeman[13] model) produces significant differences when compared to a reference probe placed in the fluidized bed. Although attenuation terms were included in the models, the potential error associated with these terms was not discussed and the authors attributed the errors to differences in the source location..

Mahan and Karchmer[14] provide a good discussion of the semi-infinite coil measurement technique with particular emphasis on gas turbine applications. The various sources of error, including a brief description regarding viscous attenuation are discussed. These authors note the dependence of viscous attenuation error on the experimental setup and recommend approaches to minimize these effects such as using shorter probes with larger diameters. However, no experimental data is provided.

Englund and Richards[15] discuss the key characteristics of designing a semi-infinite line pressure probe. However, the overall line lengths used in this study were relative short with the baseline probe design having a line length of two meters and the longest tube length being four meters. Furthermore, this work does not provide experimental verification of the transfer functions described.

In 1967, Samuelson[16] published a report that described remote pressure sensing for nuclear rocket engine testing. This report is probably the best review of the assumptions and limitations of the theory. The author provides some experimental data that shows good agreement with the theoretical models, but the frequency range of interest was less than 10 Hertz. According to Samuelson[16], Bergh and Tijdeman[13] have also shown that their segmented-line equation agrees with measured values to within 2–5 percent for a frequency range from 10-200 Hertz. Experimental data for frequencies above 200 Hertz could not be found in the open literature. Interestingly, the direct measurements of attenuation reported by Ferrara[11] suggest that discrepancies in the measured attenuation become significant for frequencies above 150 Hertz. Since most combustion instabilities occur at frequencies higher than

150 Hertz, it is important to understand the pressure measurement implications as a result of uncertainties in the attenuation factors.

B. Scope

In the ideal situation, the pressure transducer could be placed directly into the combustion environment and the errors introduced by the waveguide, or semi-infinite coil, could be avoided. However, this approach is limited by the maximum service temperature of the pressure transducer. Therefore, it is sometimes necessary to attach the pressure transducer to a remote sensing unit, such as a semi-infinite coil. Based on information available in the literature[1], a continuous gas purge is not a common practice for remote sensing units used on most gas turbine systems, and as a result the attenuation in these systems is primarily due to visco-thermal effects.

This paper will focus on the semi-infinite coil approach with no purge gas, or mean flow, through the remote pressure sensing unit. Utilizing experimental data obtained through this study, theoretically derived transfer functions relating the pressure measured in the remote unit to the desired pressure in the main body of a simulated gas turbine combustor are compared to the actual measured response. Since viscous attenuation is sensitive to surface imperfections and several other apparatus specific conditions, the data presented in this paper is specific to this experimental setup. However, these results may provide an order of magnitude estimate of the errors for remote pressure sensor configurations that incorporate a semi-infinite coil arrangement.

II. Experimental Setup

Figure 1 shows a sketch of the experimental closed-opened tube arrangement used to simulate a gas turbine combustor. A 43 cm (17 in) long, 7.6 cm (3 in) diameter commercial plastic (PVC) pipe is attached to a speaker enclosure on one end while the other end is open to the room. The remaining system components consist of a speaker (Boston Model G212), an amplifier (Realistic Model 32-2027A), and a spectrum analyzer/frequency generator (Agilent Model 35670A). Pressure s ır (P_0) and in the remote sensing unit (P_1). The sensor at station P_0 is flush-mounted in the walls of the pipe while the sensor at station P_1 is inserted into a block that orients the sensor normal to the tube wall and minimizes the volume of the transducer cavity. The volume of the transducer cavity is approximately 0.1 cm^3 which is roughly three orders of magnitude smaller than the total volume of the tubing. The inside diameter of the interconnecting tubing for the semi-infinite coil is 3.8 mm (0.15-in) and the overall length of the remote sensing unit is approximately 12.93 meters (509 in). The coil arrangement allows for the distance between P_0 and P_1 to be varied.

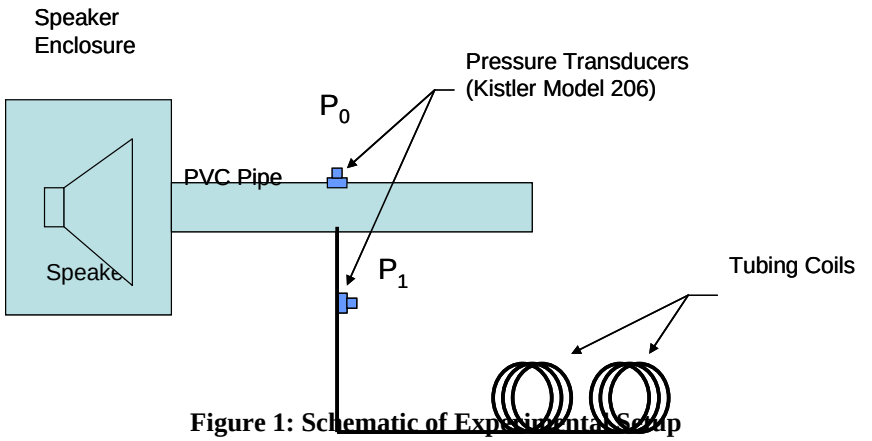

Figure 1: Schematic of Experimental Setup

The amplifier/speaker is excited using a random noise generator from the dynamic signal analyzer (Agilent 35670A). This analyzer is also used to compute the complex frequency response functions and the respective coherence functions. These functions are obtained from 150 spectral averages and the results are stored for post-processing in a MathCad program. Utilizing the coherence as a filter, data with values less than 0.98 have been rejected.

III. Data Analysis

A. Segmented Line Equation Model (Bergh and Tijdeman[13])

This model is an extension of the work of Iberall[17] (1950) and is considered by others[12,16] to be the best approach for this type of problem. Samuelson[16] provides a good overview of the assumptions required to simplify Bergh and Tijdeman's generalized segmented-line equation into the expression shown in Eq. 1. The key assumption is that the tubing is homogeneous everywhere, except at the transducer tap.

$$\frac{P_1}{P_0}(i\omega) = \left[\cosh(yL_{01}) + Q\sinh(yL_{01}) + \left(\sinh(yL_{01})\tanh(yL_{1e})\right)\right]^{-1} \tag{1}$$

The volume of the transducer cavity, V, is incorporated into the reflection coefficient, Q. According to Samuelson[16], the reflection coefficient for an adiabatic expansion in the transducer cavity can be expressed as shown in Eq. 2. Zero and first order Bessel Functions are denoted by J_0 and J_1, respectively. The arguments for the Bessel Functions are the dimensionless shear wave number, W, (see Eq. 3) and the product of the shear number and the Prandtl Number, E (see Eq. 4). Note that the value of Q becomes more significant as product of the transducer volume and the frequency increases given a constant cross-sectional area of the interconnecting tubing, A, and speed of sound, c.

$$Q = \frac{\omega V}{cA}\left[\frac{1}{\left[1+\frac{2(\gamma-1)\cdot J_1(E)}{E\cdot J_0(E)}\right]\cdot\left[\frac{2\cdot J_1(W)}{W\cdot J_0(W)}-1\right]}\right]^{\frac{1}{2}} \tag{2}$$

$$W^2 = R^2\cdot\left(\frac{-i\omega\rho}{\mu}\right) = R^2\left(-\frac{i\omega}{\nu}\right) \tag{3}$$

$$E = \Pr\cdot W \tag{4}$$

The second parameter in Eq. 1 that must be defined is the propagation constant, y (see Eq. 5). Although Samuelson[16] describes simplifications to these expressions depending on the range of shear numbers expected in the problem, none of these simplifications will be used in the analysis presented below.

$$y = \frac{\omega}{c}\cdot\left[\frac{1+\frac{2(\gamma-1)\cdot J_1(E)}{E\cdot J_0(E)}}{\frac{2\cdot J_1(W)}{W\cdot J_0(W)}-1}\right]^{\frac{1}{2}} \tag{5}$$

It should be noted that the term in square brackets represents the attenuation due to visco-thermal effects. This attenuation term is composed of an imaginary and a real component. The imaginary component is sometimes called the phase-shift coefficient, and the real component is called the attenuation coefficient. This will be described in more detail in the next section.

B. Viscous Attenuation Terms

As previously mentioned, viscosity and heat loss effects are the primary attenuation mechanisms for sound waves propagating through small diameter tubes containing a stationary media. It is interesting to note that these visco-thermal loss coefficients are not always reported consistently in introductory acoustic textbooks. For example, Munjal[10] and Kinsler[18] have slightly different expressions for the visco-thermal attenuation coefficient and both of these expressions differ from the attenuation coefficient (the real component of the term in the square brackets) of Eq. 5. Figure 2 shows a comparison between the attenuation coefficients from Munjal[10], Kinsler[18], and Samuelson[16]. Note that the expressions from Munjal[10] and Kinsler[18] have been normalized by the wave number (i.e., ω/c) to express them in dimensionless form. All three expressions agree for large shear wave numbers (i.e. W>30) where viscous damping is very low. However, for the experimental setup described in this paper, the frequency range of interest is 100-800 Hertz and the corresponding shear wave numbers are in the range of 10-30. Therefore, Eq. 5 will be used.

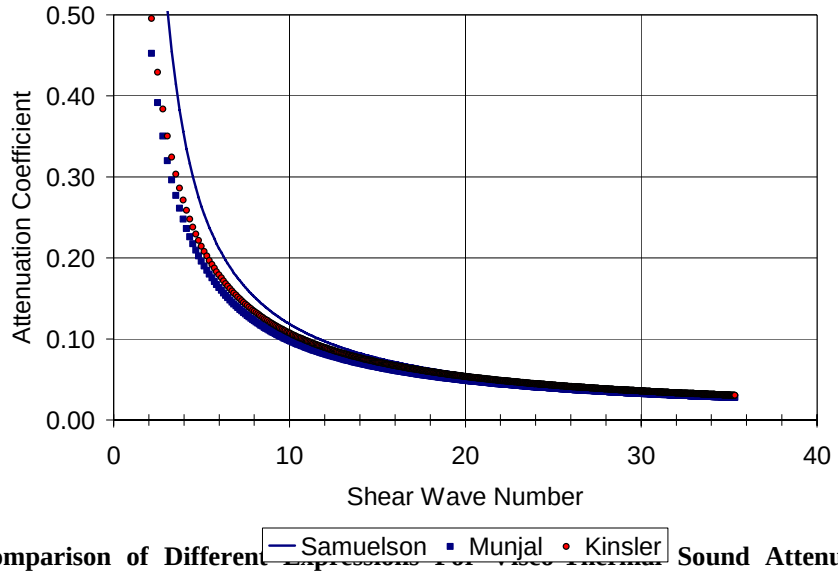

Figure 2: Comparison of Different Expressions For Wave Thermal Sound Attenuation in Tubes with Circular Cross-Section

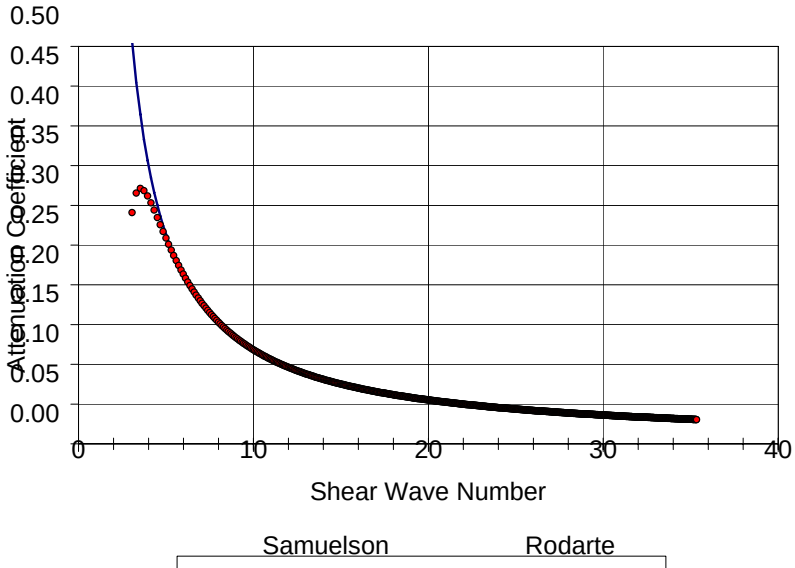

Figure 3: Comparison of Attenuation Coefficient With Bessel Functions To Curve-Fit Developed By Rodarte et. al[19]

It is interesting to note that a polynomial fit for the attenuation coefficient has been developed by Rodarte et. al[19]. This curve fit is applicable for a wide range of gases and does not involve Bessel Functions. Figure 3 shows a comparison between Rodarte's curve-fit and the attenuation coefficient that can be obtained from Eq. 5. Note that the curve-fit begins to deviate for shear wave numbers less than about six. For the configuration studied in this paper, this corresponds to frequencies of less than 10 Hertz which was outside the low frequency cutoff for the speaker.